Altogether Archaeology

Gueswick Hills, Teesdale
Fluxgate Gradiometer Survey

June 23rd, 2019

Contents

Copyright & Acknowledgments

Copyright

Editors

Stephen Eastmead, Martin Green and Rob Pearson.

Images and Maps

Should be credited to Stephen Eastmead.

Google Earth Image © Google 2018

Acknowledgements

Swaledale and Arkengarthdale Archaeology Group for their generous use of their GPS and Bartington equipment, and to Mike Keenan and Mike Walton for their enthusiasm, time and assistance. https://swaag.org/index.php#

Ordnance Survey:

1. https://www.ordnancesurvey.co.uk/opendatadownload/products.html
2. https://www.ordnancesurvey.co.uk/gps/os-net-rinex-data/

Environment Agency Data https://environment.data.gov.uk/DefraDataDownload/?Mode=survey

Land Access

Whilst there are public footpaths nearby, there is no public access to the survey area.

Website

https://altogetherarchaeology.org/

Cover Image

Cover Image: Gueswick Hills (NZ 0036 2104) looking east at the survey area.

The cover image is also shown right with the four magnetometry sites indicated.

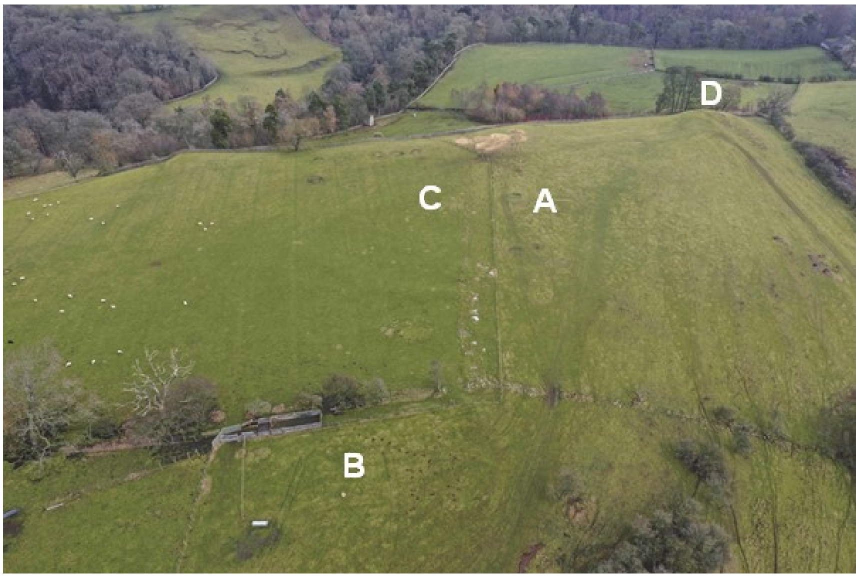

Introduction

An Altogether Archaeology member suggested looking at this Gueswick Hills site as a survey area which may have potential for further archaeological examination. With the landowner's permission Altogether Archaeology walked over the site in early 2019.

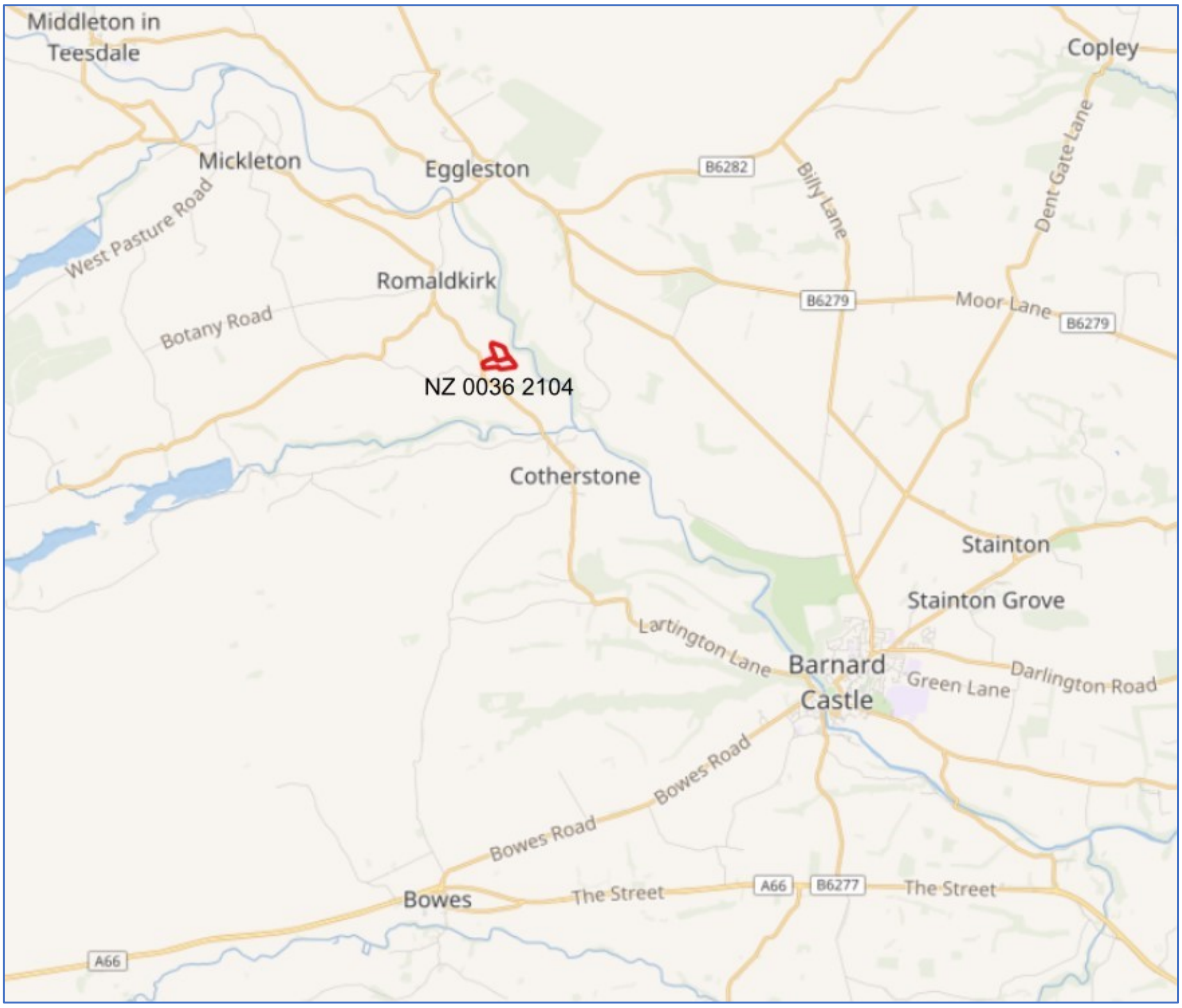

Figure 1: Gueswick Hills are located mid-way between Cotherstone and Romaldkirk near Barnard Castle, County Durham. Prior to the 1974 boundary changes this site was in North Yorkshire

Figure 2: Gueswick Hills Promontory

The predominant archaeological evidence is the extensive rig and furrow ploughing and a significant number of cultivation terraces. Gueswick Hills are one of a series of glacial terminal moraines found across the River Tees valley. The soil is very sandy with no watercourses. The nearest watercourse, Wilden Beck, is at an elevation between 170 m – 180 m whereas the study area is between 210 m – 223 m. The River Tees is around 160 m – 170 m above mean sea level. Not surprisingly, there is no obvious evidence of settlement. However, as Gueswick Hills form a significantly raised promontory above the surrounding landscape

(Figure 2), it must be a reasonable candidate to find some indications of prehistoric activity being present. There is a cairn beside Site B (Figure 5) and a single earth-fast stone that has been reported as having been carved with 'Rock Art', which is not very convincing. The County Durham HER does not contain any records on the top of Gueswick Hills inside the survey area. But at the western end in an adjacent field, there is a medieval stone cross base built into a drystone wall next to a public footpath stile, situated on the north side of the B6277 Cotherstone to Romaldkirk road. It was one of two surviving cross-bases on the old route from Cotherstone to Romaldkirk church, along which bodies were carried for burial.

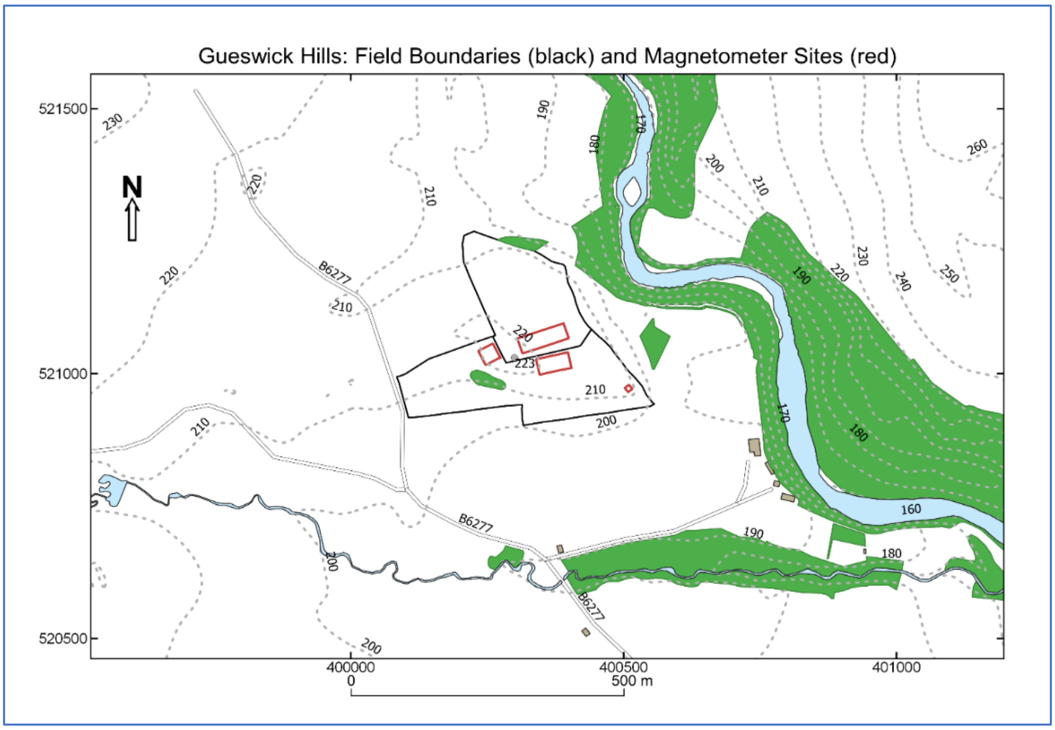

Figure 3: Gueswick Hills map showing field boundaries (black) and four magnetometer sites (red)

The conclusion of the walk-over survey was to select four areas on top of the promontory to examine using a Fluxgate Gradiometer to measure the soils magnetic susceptibility within those four areas. The four sites are outlined in red on Figure 3.

Survey Sites

The three-dimensional form of the Gueswick Hills promontory and its relationship with the surrounding landscape are best seen in the lidar image (Figure 4).

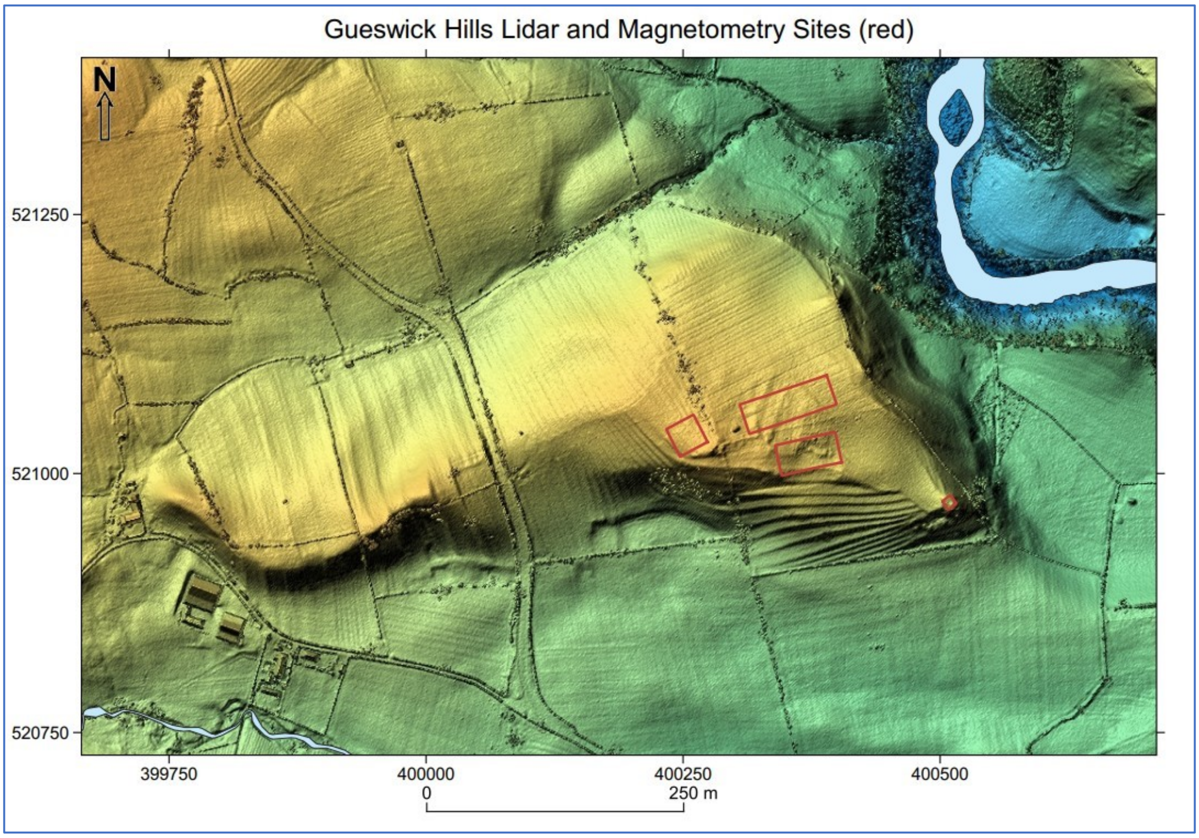

Figure 4: Gueswick Hills Lidar

The four sites chosen for magnetometry were identified as A, B, C & D as shown in Figure 5.

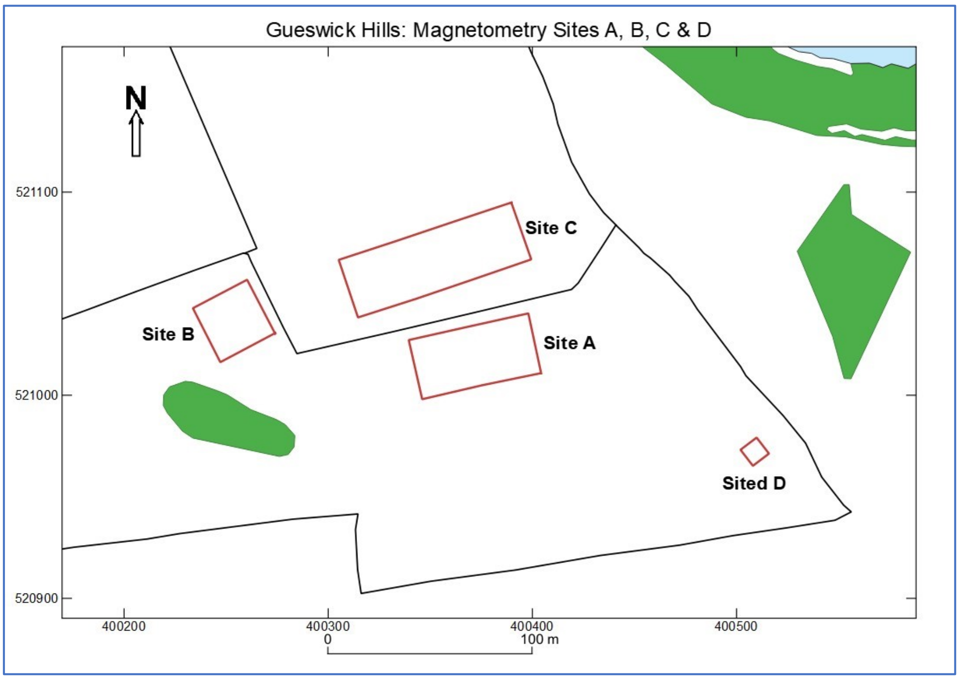

Figure 5: Magnetometry Sites A, B, C & D

Sites A, B & C Lidar

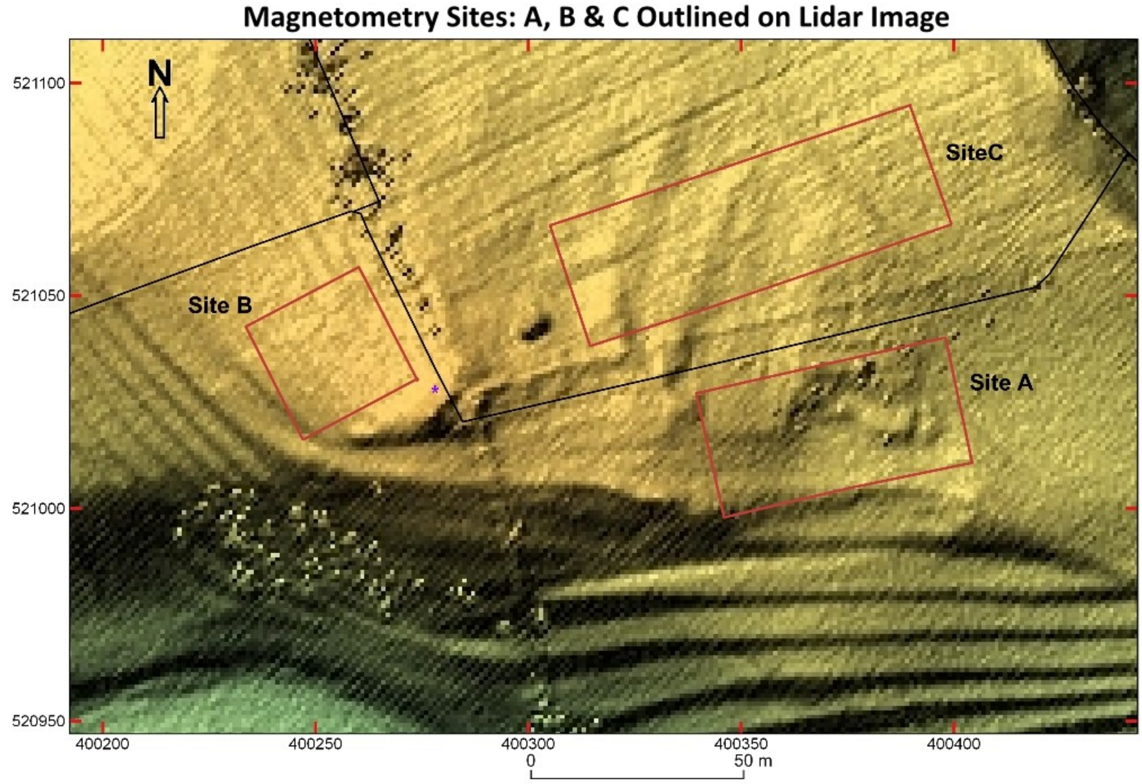

Figure 6: Lidar image for Sites A, B & C

Site A

Figure 7: Site A next to wire fence

Site A was selected because it contained the only area of significant earthworks, which are of irregular shape. The black lines on Figure 6 are modern wire fence-lines. Whilst the outer field boundaries were of dry-stone wall construction for the most part, the inner fences close to the three sites A, B & C were all wire. Between the wire fence separating Site A from Site C and Site C, is a grassed over foundation of a dry-stone wall, which makes a 90° turn south crossing over the terracing towards the bottom of the lidar image. The Site A survey grid measures 30 m x 60 m and was sited a respectful distance away from the wire fence.

Site B

Figure 8: Site B next to the cairn by the wire fence

Site B is a 30 m x 30 m grid. Figure 6 shows a small purple asterisk just beside the grid's eastern most corner which marks the centre of the cairn. The cairn can be seen in Figure 8 just beyond the corner of the wire fence.

The grid couldn't be placed either further north or east due to the presence of metal gates, an animal pen and wire fences.

Site C

Figure 9: Site C in the foreground. The River Tees is in the valley amongst the trees on the right

The Site C grid measured 90 m x 30 m. The placement leaves a gap between the western fence-line and the western end of the grid C (Figure 6). This was due to that area being used to bury farm animals in the past when that was a permitted practice. The oval area on the lidar may well be the location of the pit.

In addition, somewhere around that area a farm building has been demolished. It is possible that the western end of the grid may still be on top of that building. The circles on the Site C image (Figure 9) are from the use of Round Bale Ring Feeders used to feed cows their winter hay/silage.

Site D

Site D is a 10 m x 10 m grid located on the eastern promontory headland (Figures 10 & 11).

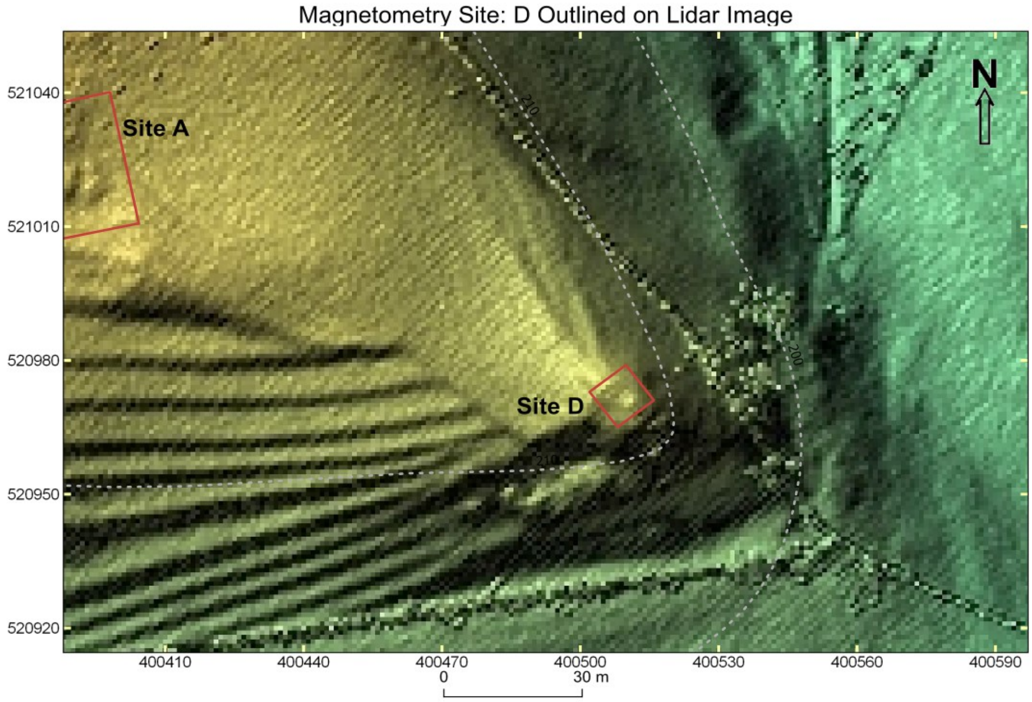

Figure 10: Site D Lidar

Figure 11: Site D

The 10 m x 10 m grid normally has limited value but due to the sharp drop-off on 3 sides that was the best that could be done. Its function was just to see if there was any sign of archaeological use of this prominent geological feature.

Methodology

Introduction

A Fluxgate Magnetometer is used to determine the how magnetic the topsoil layers are. This technique relies on topsoil containing different amounts of various iron oxides, which become magnetised in the earth's magnetic field (magnetic susceptibility).

There are many forms of iron oxide [https://en.wikipedia.org/wiki/Iron_oxide]. Different forms of iron oxide can be magnetised to varying degrees. Conversion of a weakly magnetised form to a stronger magnetic form can occur by both heat (thermoremanence) and by various bacterial fermentation processes that can occur when the soil conditions are right. The common example often quoted is when oxygen is excluded and the resulting reducing conditions lead to a conversion of the soil's weakly magnetically susceptible haematite (α-Fe_2O_3), to magnetite (Fe_3O_4), with a strong increase in magnetic susceptibility.

This technique relies on topsoils types being naturally more magnetic than subsoils. For example, if a ditch is excavated down into the subsoil and then over a period it naturally fills with more magnetically susceptible topsoil sediments, and / or a greater topsoil depth. Then the Fluxgate Gradiometer will detect a higher reading when it crosses over the ditch compared with the ground on either side of the ditch.

Human habitation can enhance magnetic susceptibility by creating open fires, ovens, furnaces or by burying waste in middens which can become an anaerobic fermentation site as they 'compost' the waste.

The Fluxgate Magnetometer (Bartington 601-2) has a pair of Fluxgate detection tubes 1 metre apart. Each tube has two sensors, one at the bottom of the tube and the second at the top. The top sensor measures the Earth's magnetic field whilst the lower sensor measures both the earth's magnetic field strength and that of the soil. The topsoil's reading can then be obtained by subtraction of the top sensor's reading from the bottom sensor's reading. The magnetic field is measured in nanotesla units (nT).

Instruments

- ProMark 120 GPS using 1-minute Rinex OS-Net correction data. #
- Bartington 601-2 Gradiometer. #

Data Processing

- Spectra Precision Survey Office #
- TerraSurveyor #
- QGIS
- GPS Utility
- DrawPlus

Swaledale and Arkengarthdale Archaeology Group equipment (http://swaag.org).

Site Results

Site A

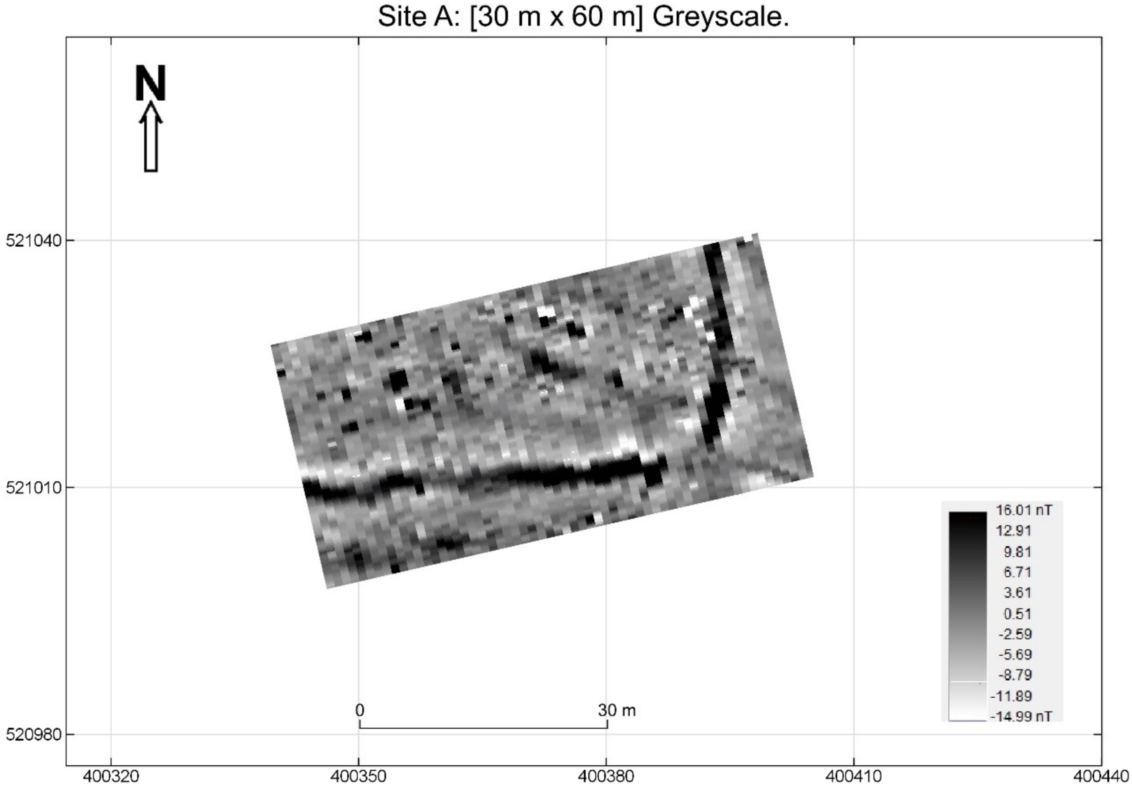

Figure 12: Site A Greyscale Image

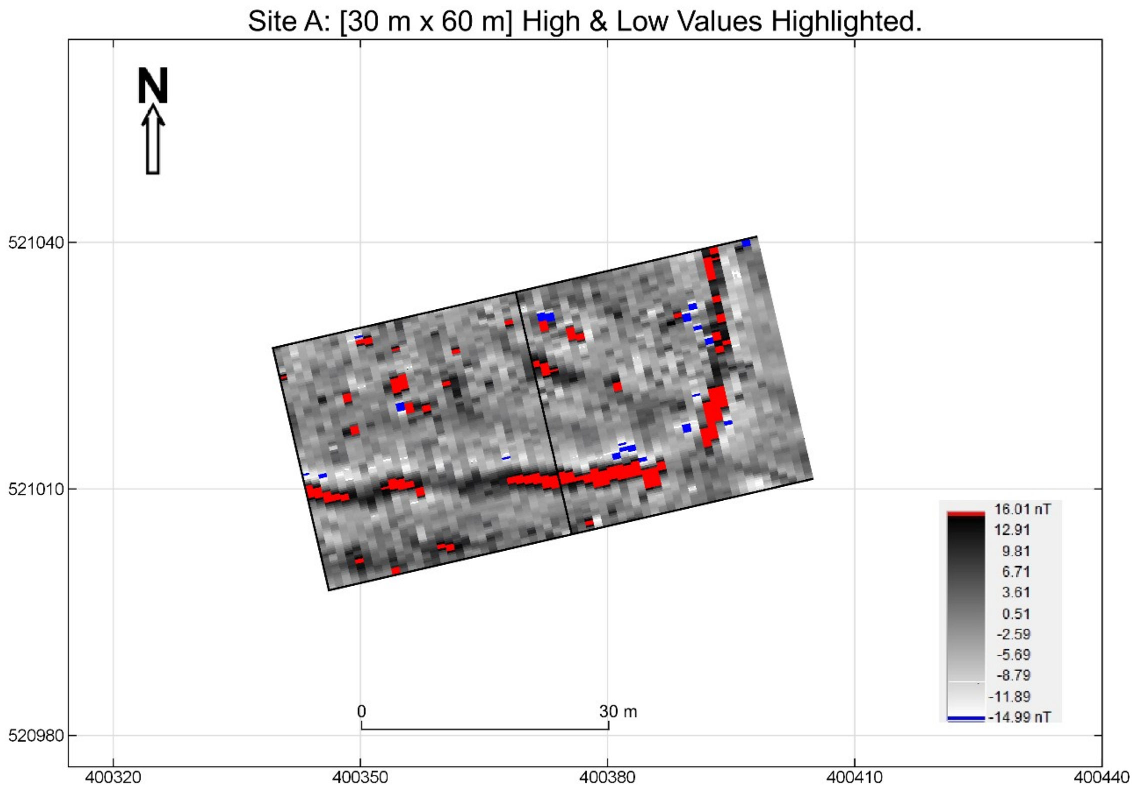

Figure 13: Site A Greyscale with High (red) and Low (blue) readings highlighted

Site B

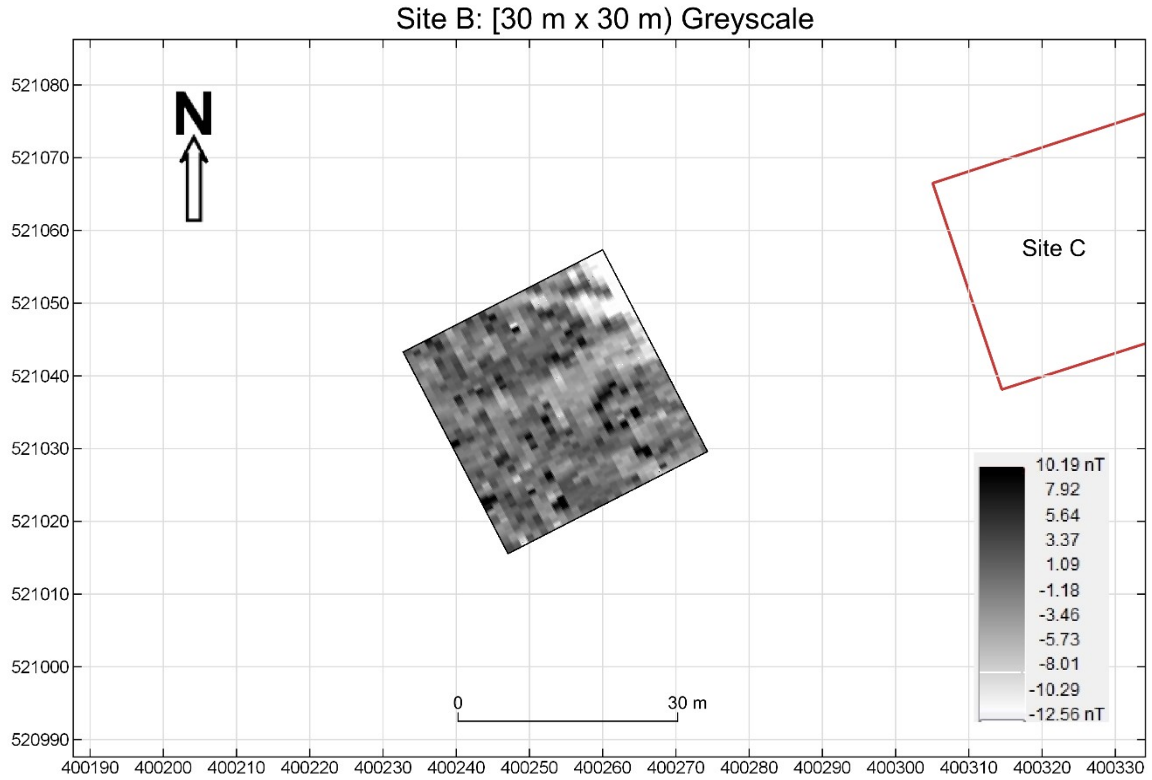

Figure 14: Site B Greyscale Image

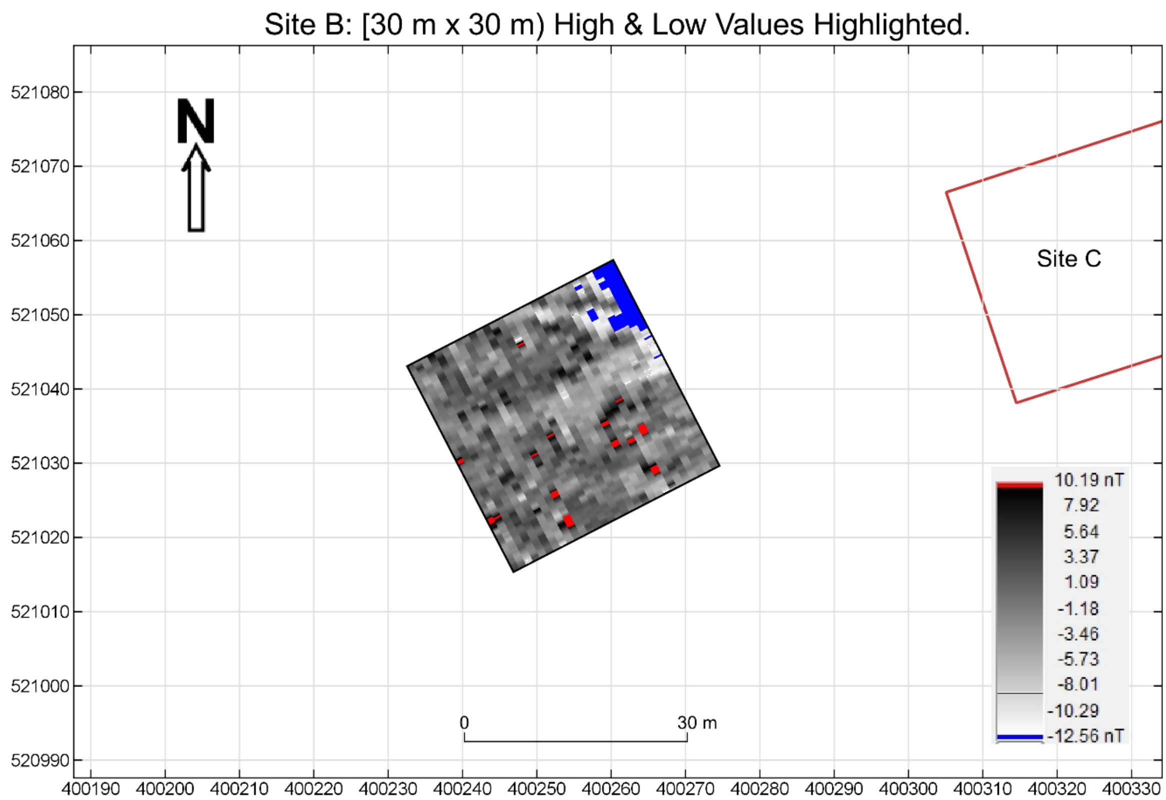

Figure 15: Site B Greyscale with High (red) and Low (blue) readings highlighted

Site C

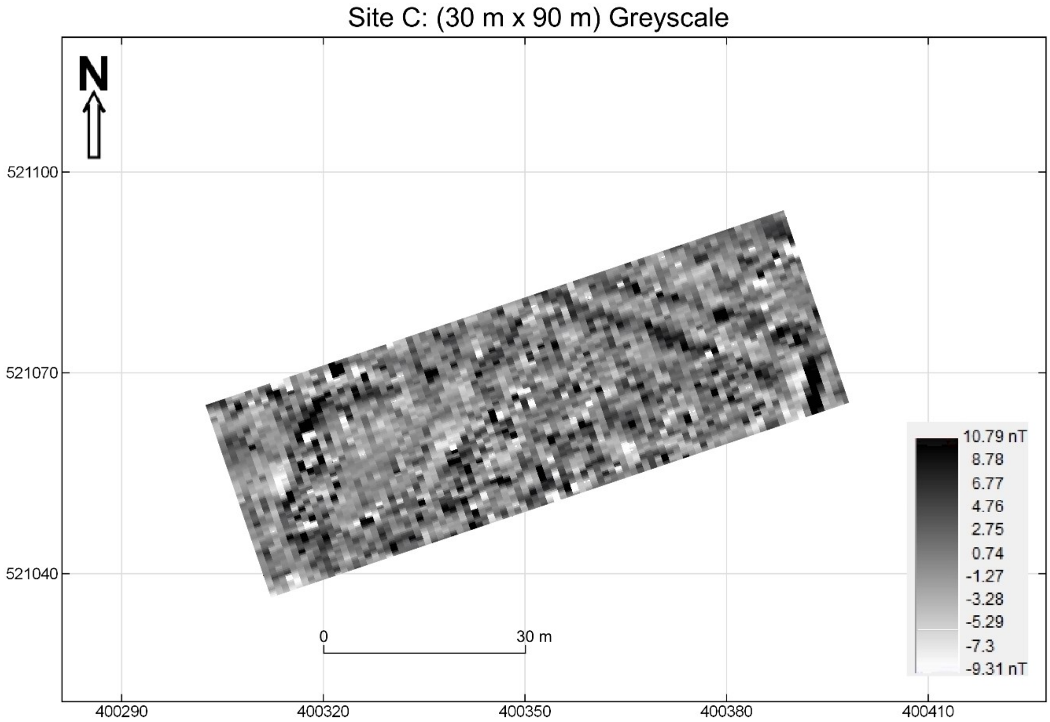

Figure 16: Site C Greyscale Image

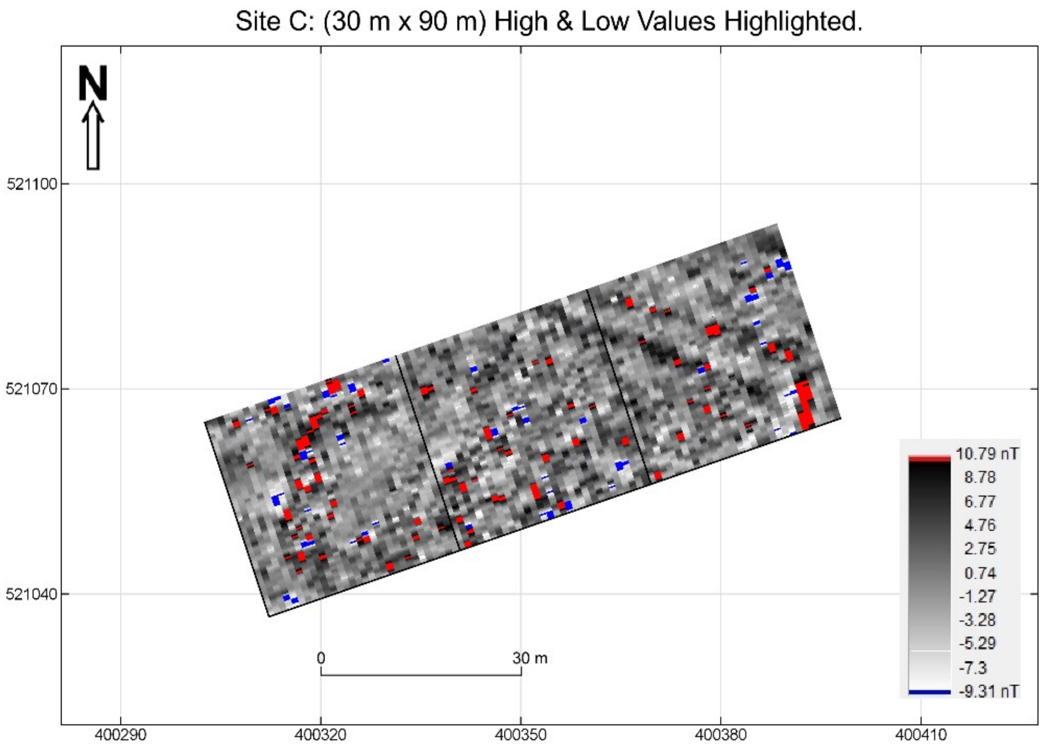

Figure 17: Site C Greyscale with High (red) & Low (blue) readings highlighted

Site D

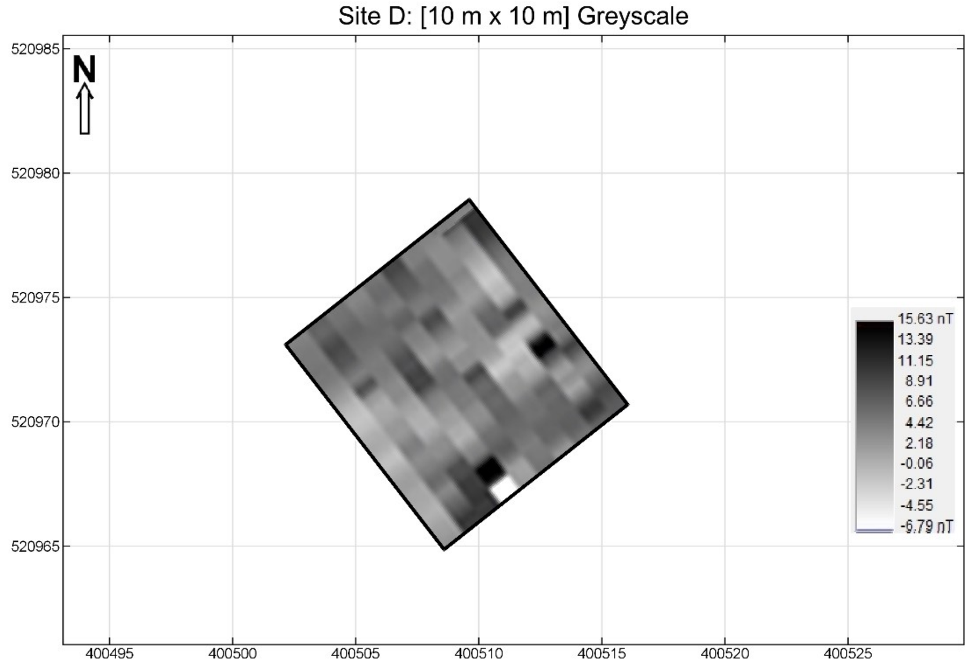

Figure 18: Site D Greyscale Image

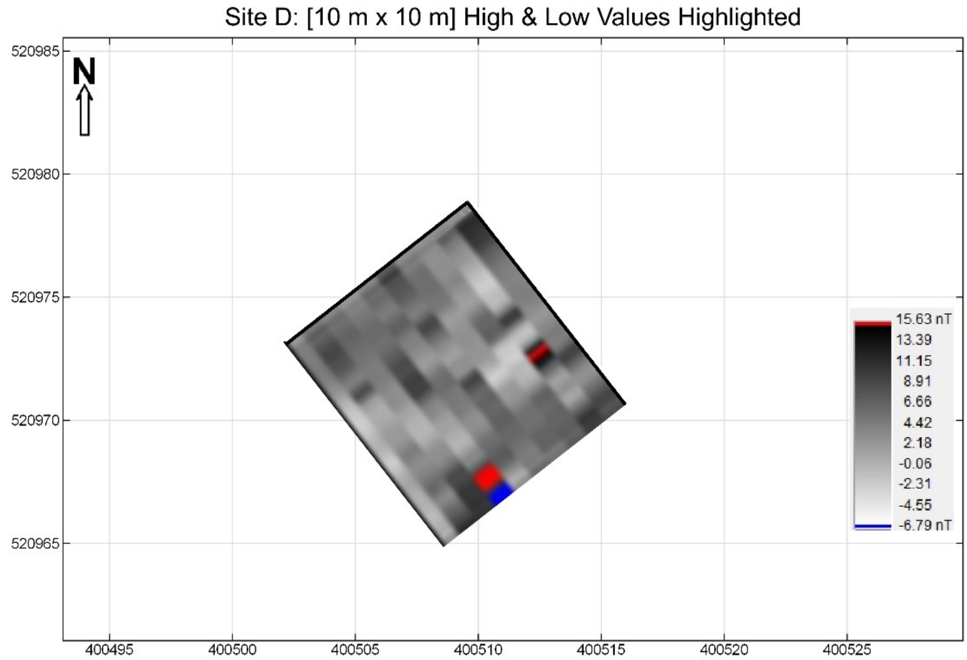

Figure 19: Site D Greyscale with High (red) & Low (blue) readings highlighted

Sites A & C Magnetometry and Lidar

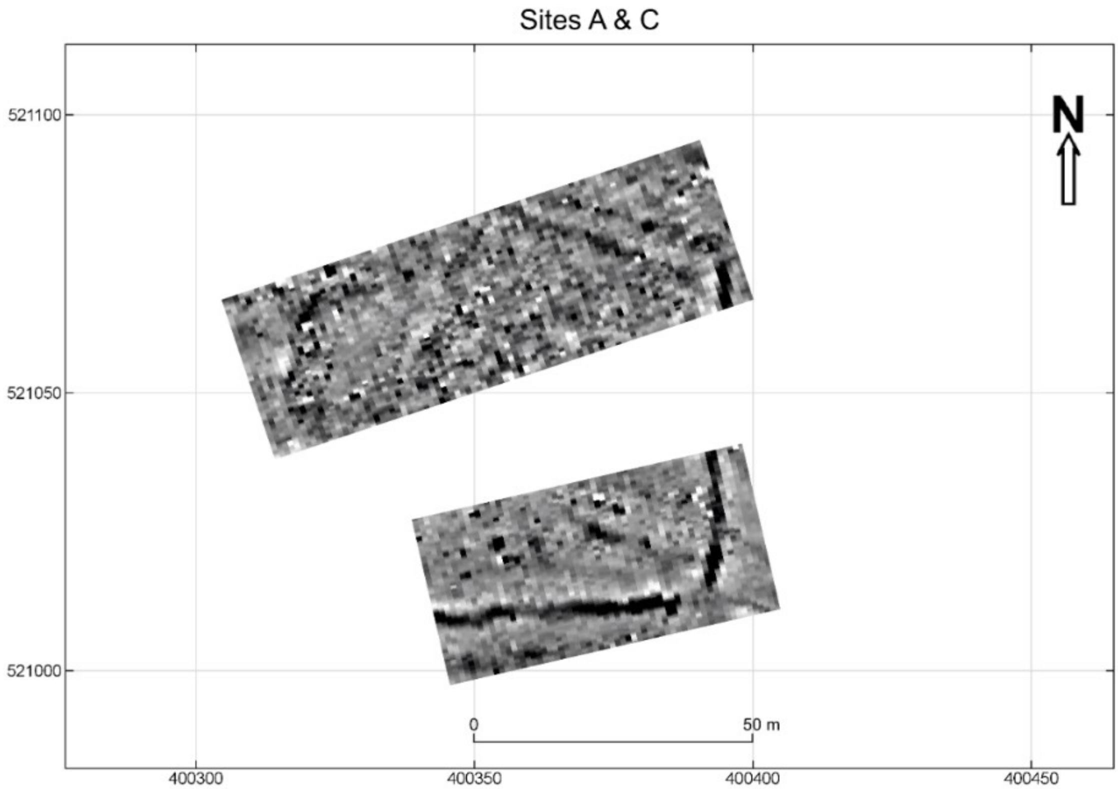

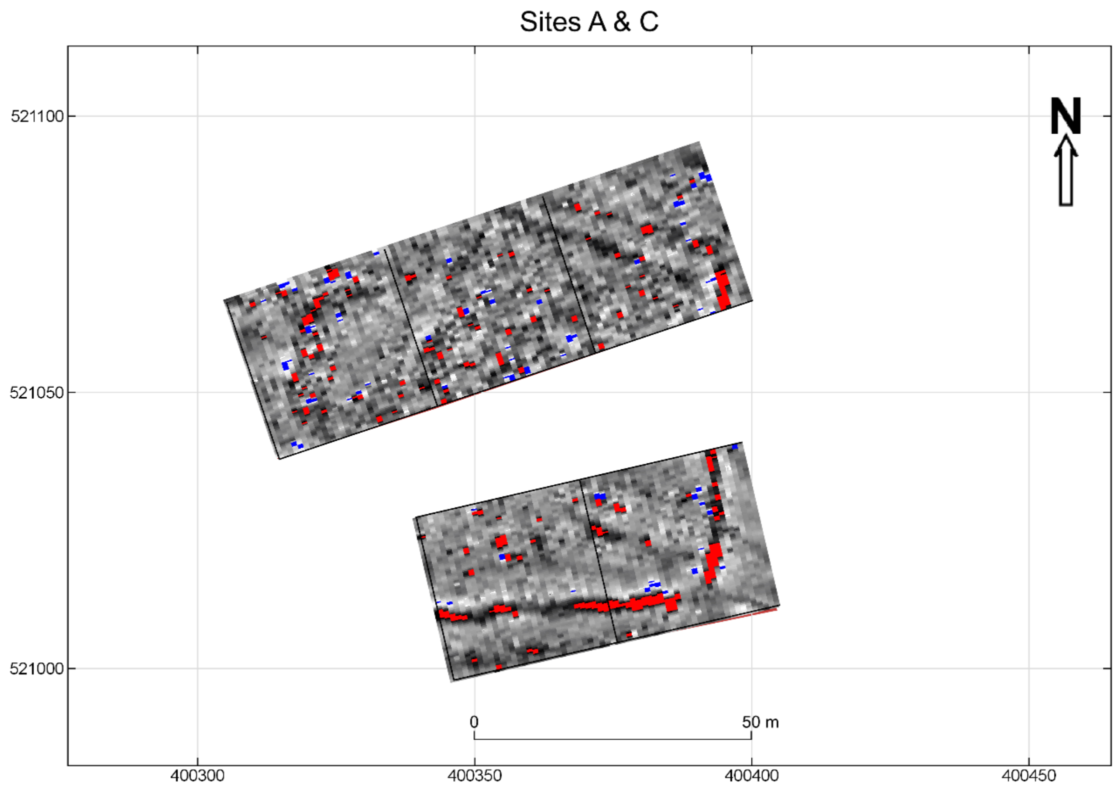

Figure 20: Sites A & C Magnetometry

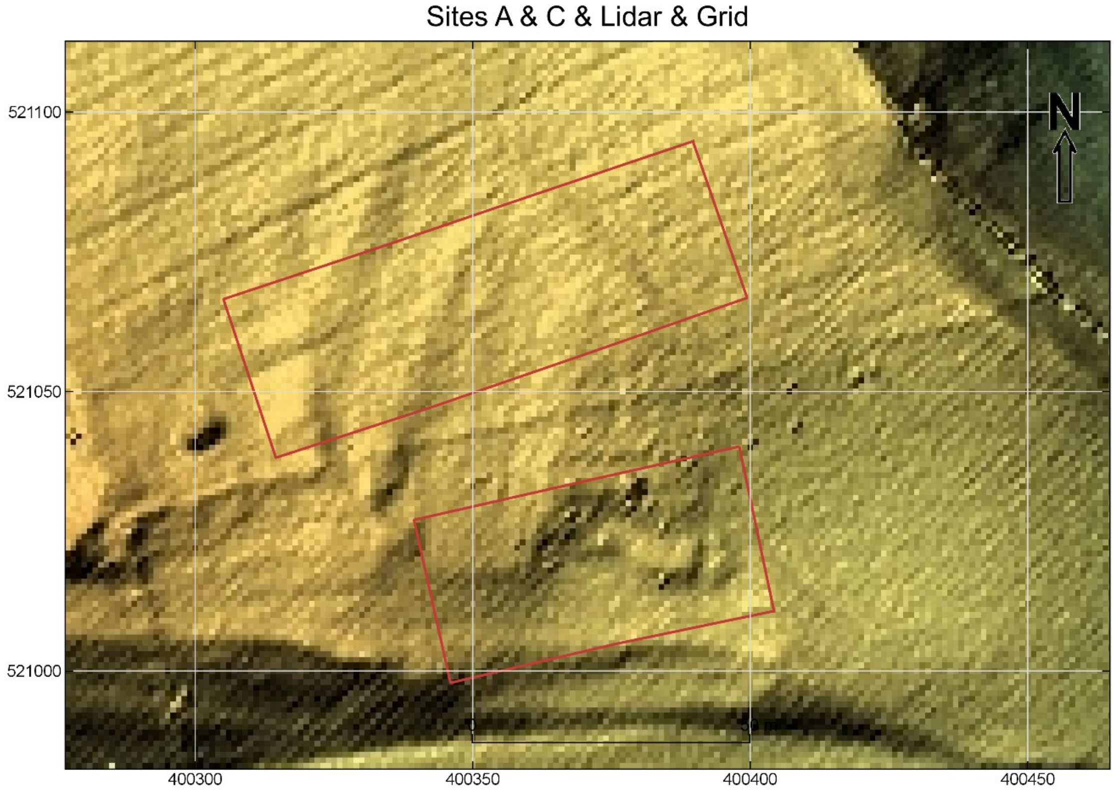

Figure 21: Sites A & C Position on Lidar

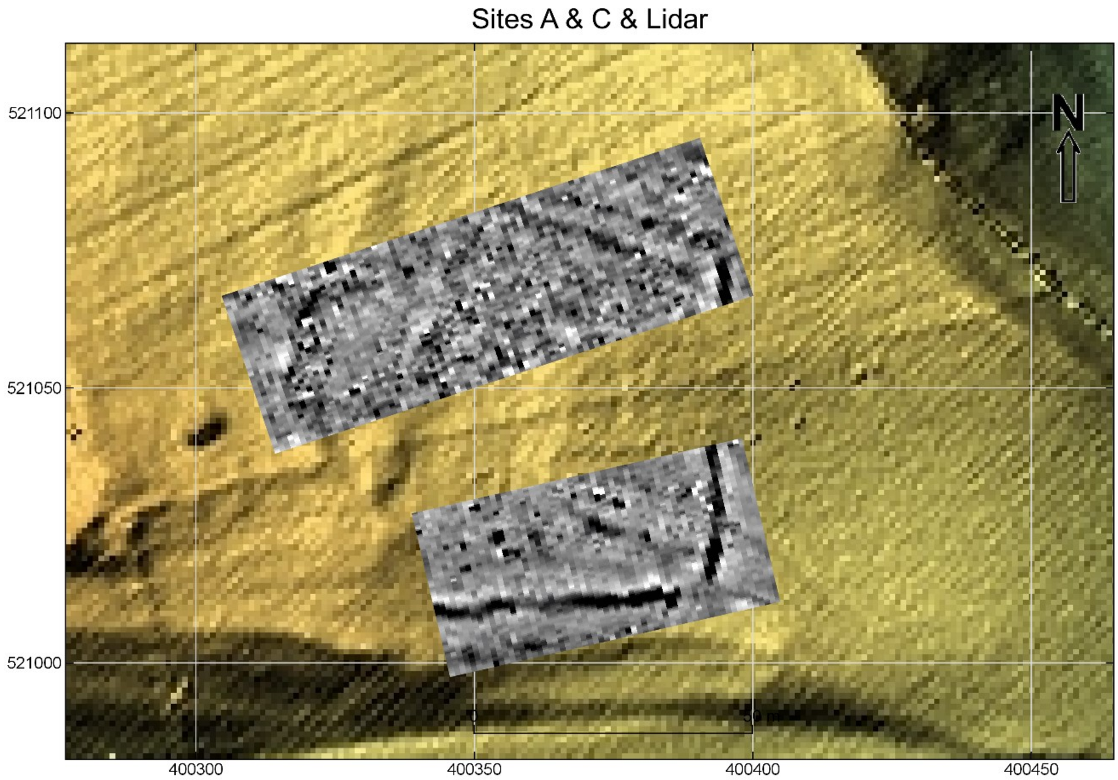

Figure 22: Sites A & C Magnetometry on Lidar

Interpretive Maps

Site A

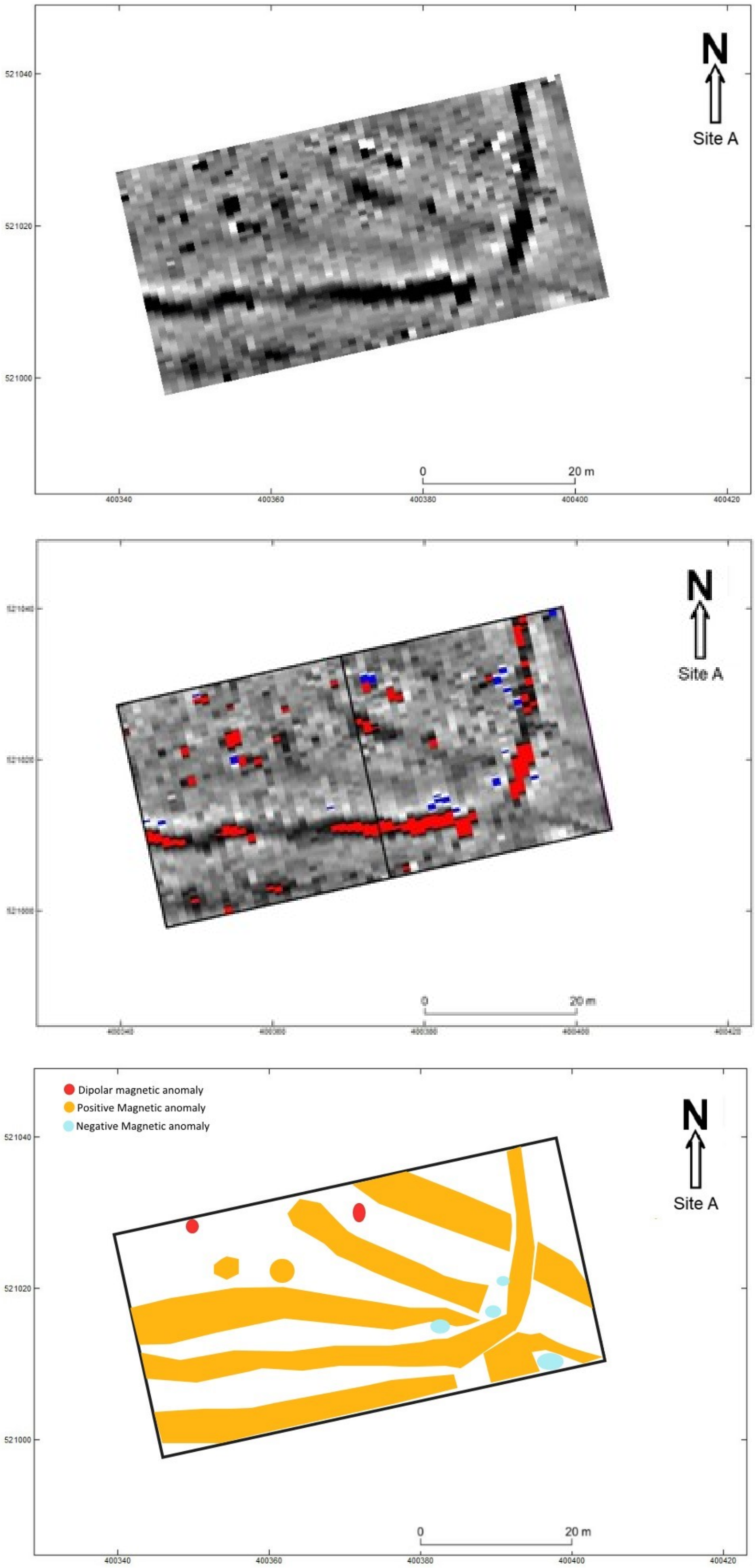

Figure 23: Site A - Interpretive Images

Site B

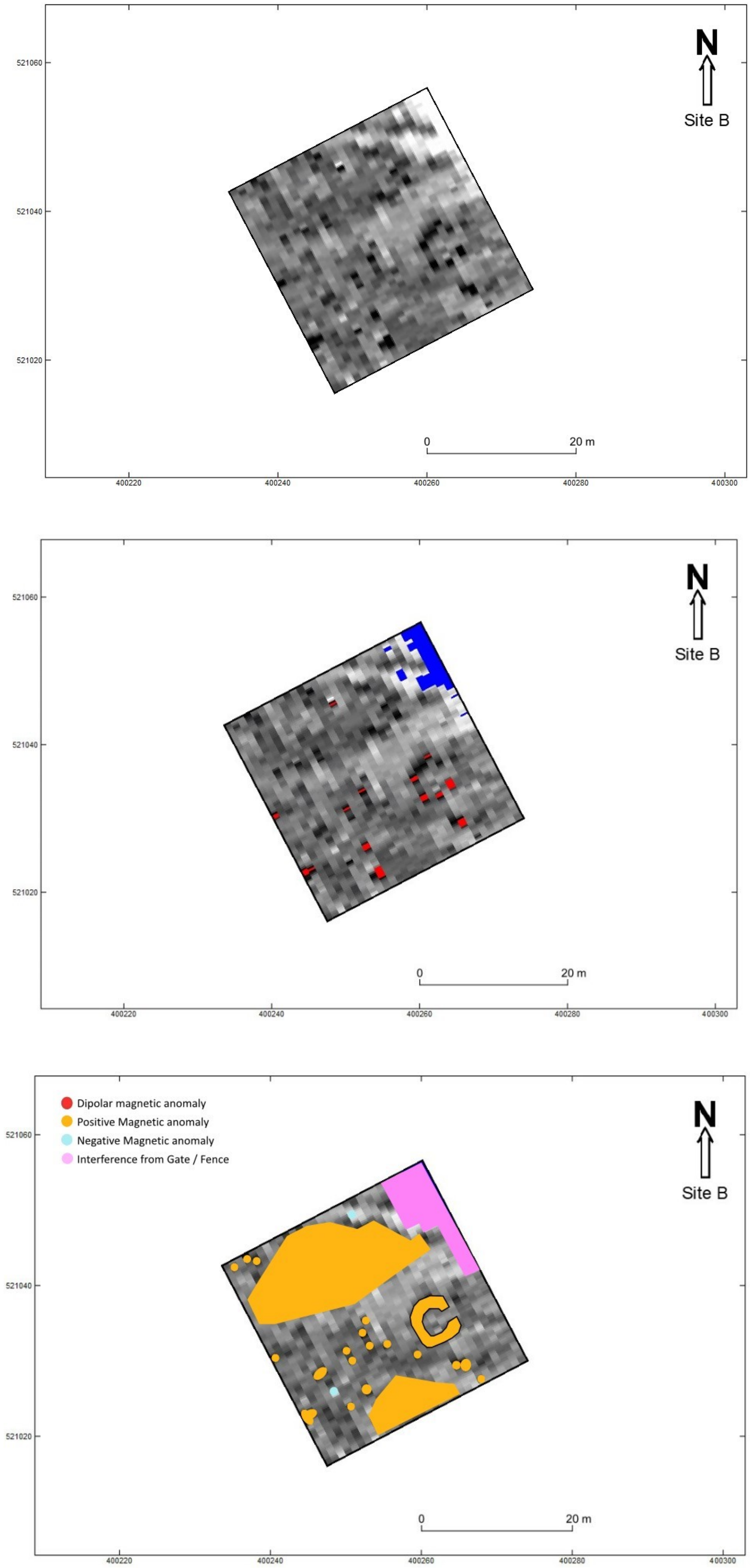

Figure 24: Site B – Interpretive Images

Site C

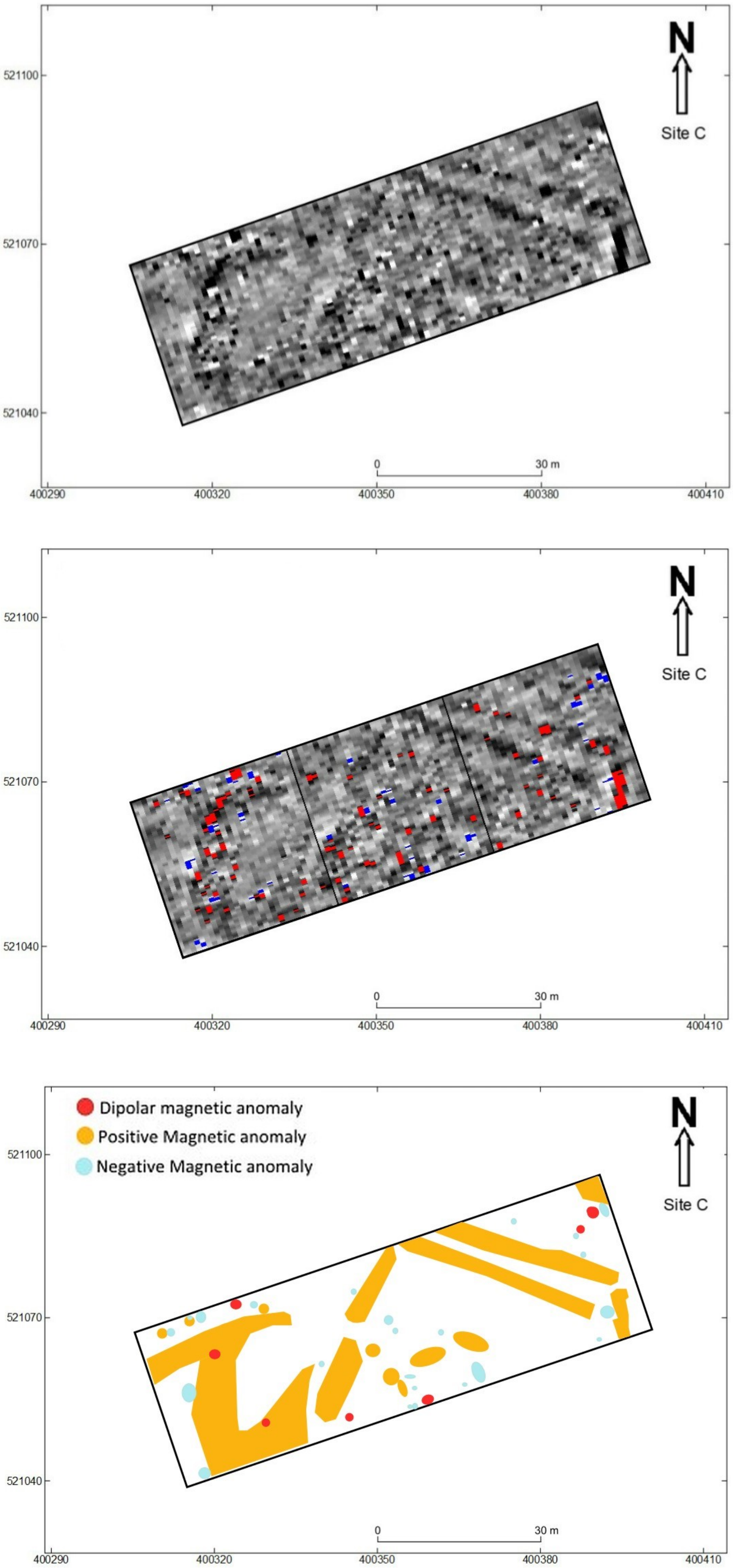

Figure 25: Site C – Interpretive Images

Site D

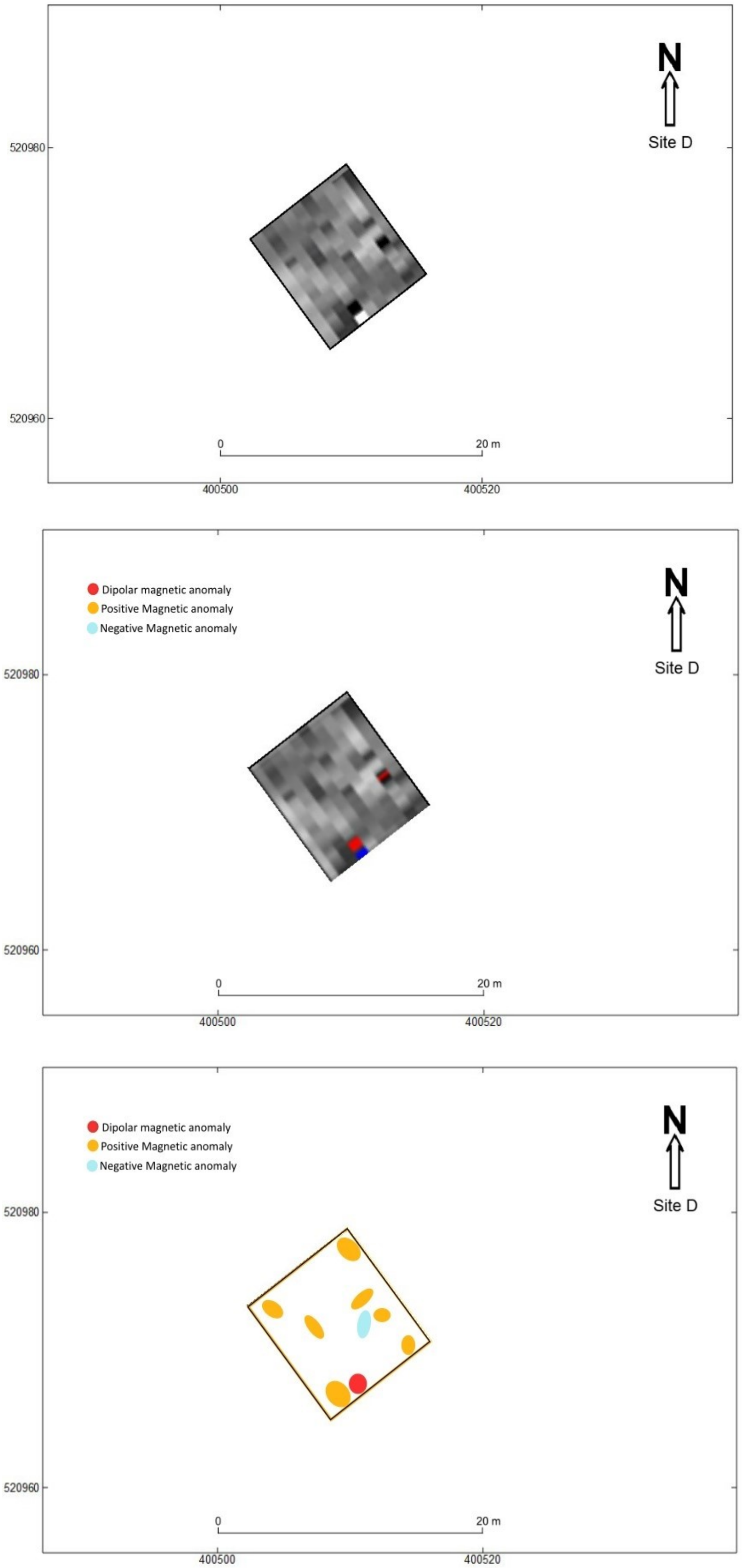

Figure 26: Site D – Interpretive Images

Interpretation: Anomaly Types

Three general types of geomagnetic anomalies:

- Positive magnetic regions of anomalously high or positive magnetic field gradient, which may be associated with high magnetic susceptibility soil-filled structures such as pits and ditches.
- Negative magnetic regions of anomalously low or negative magnetic field gradient, which may correspond to features of low magnetic susceptibility such as wall footings and other concentrations of sedimentary rock or voids.
- Dipolar magnetic paired positive-negative magnetic anomalies, which typically reflect ferrous or fired materials (including fences and service pipes) and/or fired structures such as kilns or hearths.

Anomalies can arise from geological processes as well as human activity. Geological anomalies tend to be broader and less well defined than those caused by human activity. The signal strength measured will not only be dependent on its magnetic susceptibility in the Earth's magnetic field, but on its depth in the soil. Whilst most ditches and pits give a positive magnetic field gradient, there is no reason why they could not have been filled with low magnetically susceptible soils.

Conclusions

Site A

Site A was a 30 m x 60 m grid. The lidar image (Figure 6) shows an irregular earthwork towards the eastern half of the grid, with a suggestion of a small rectangular feature near its centre. The southern length marking the plateau of a series of south facing terraces. The north west corner shows a slightly elevated feature that appears to run NNE extending through Site C. This raised feature predates both the wire fence and the earlier dry-stone wall foundation, and possibly the rig and furrow ploughing too.

The most intense magnetic anomaly follows the top of the plateau and then turns northwards toward the NE corner of the grid. This north-eastwards section looks like a ditch on the lidar which would be consistent with this type of magnetic anomaly. This anomaly appears to extend through into the SE corner of Site C before continuing westwards in Site C as it weakens in intensity.

There are four weak positive anomalies that traverse the grid in broadly in an east west direction. Two of these anomalies pass through the SW corner of the intense anomaly described above. This appears to be potentially a complex area.

Site B

Site B was a single 30 m x 30 m grid sited close to the cairn. A farm animal pen next to the north-east corner of the grid caused magnetic interference to that area (Figure 24).

There is a suggestion of a 'C' shaped feature towards the south-east corner of the grid together with a scatter of small high readings.

The lidar image doesn't show any archaeological features (Figure 6).

Site C

Site C was a single 30 m x 90 m grid situated just north of Site A. The lidar (Figure 6) shows not only that features extend from Site A into Site C but also beyond Site C to the north. As described in Site A, an intense positive anomaly extends from Site A northwards into the SE corner of Site C where it makes a left-hand turn NW extending beyond the northern boundary of the grid. There is a second slightly more intense magnetic anomaly running nearly parallel and slightly south of the previously described anomaly. This anomaly also extends beyond the northern grid boundary.

There is a weak positive magnetic anomaly running from the centre of the northern edge of Site C south-westwards. If it extended through to the area immediately to the west of Site A, then it may be the return ditch completing the main feature as a rhomboidal enclosure.

At the western end of Site C are further areas of moderately intense positive anomalies. A building was apparently demolished somewhere in the corner of this field. However, the only Ordnance Survey map that shows buildings in this area is shown in Figure 27 below. The main building on the map appears to be located over the cairn (very unlikely), and a second structure of narrow appearance, appears to be in Site A's field and not in Site C's field.

Figure 27: OS 1940-1953 Survey Map

Site D

Site D was a single 10 m x 10 m grid located on the small headland. No significant features were detected (Figure 26). The lidar image also doesn't show any archaeological features (Figure 10).

Summary

Both Site A and Site C grids appear to contain quite complex archaeological anomalies which are likely to be of a multi-period nature. Some features appear in both the lidar and magnetometry images. They appear to be worthy of further archaeological investigation.

Sources

- Gaffney, C, & Gater, J, 2003 Revealing the Buried Past, Tempus.
- Clark, A, 1990, Seeing Beneath the Soil, Batsford Book.
- Eastmead, S, Use of QGIS Graphical Information System in Basic Field Archaeology and Lidar Processing (pdf download), https://www.eastmead.com/QGIS-LIDAR.htm